HHS Public Access

Author manuscript

Kidney Int. Author manuscript; available in PMC 2017 May 09.

Published in final edited form as:

Kidney Int. 2017 February ; 91(2): 338–351. doi:10.1016/j.kint.2016.09.017.

Generation and phenotypic analysis of mice lacking all urea transporters

Tao Jiang, Ph.D.[#],
State Key Laboratory of Natural and Biomimetic Drugs, Department of Pharmacology, School of Basic Medical Sciences, Peking University, Beijing, 100191, China

Yingjie Li, M.S.[#],
State Key Laboratory of Natural and Biomimetic Drugs, Department of Pharmacology, School of Basic Medical Sciences, Peking University, Beijing, 100191, China

Anita T. Layton, Ph.D.,
Department of Mathematics, Duke University, Durham, North Carolina 27708, USA

Weiling Wang, Ph.D.,
State Key Laboratory of Natural and Biomimetic Drugs, Department of Pharmacology, School of Basic Medical Sciences, Peking University, Beijing, 100191, China

Yi Sun, Ph.D.,
State Key Laboratory of Natural and Biomimetic Drugs, Department of Pharmacology, School of Basic Medical Sciences, Peking University, Beijing, 100191, China

Min Li, Ph.D.,
State Key Laboratory of Natural and Biomimetic Drugs, Department of Pharmacology, School of Basic Medical Sciences, Peking University, Beijing, 100191, China

Hong Zhou, Ph.D., and
State Key Laboratory of Natural and Biomimetic Drugs, Department of Pharmacology, School of Basic Medical Sciences, Peking University, Beijing, 100191, China

Baoxue Yang, Ph.D.[*]
State Key Laboratory of Natural and Biomimetic Drugs, Department of Pharmacology, School of Basic Medical Sciences, Peking University, Beijing, 100191, China; Key Laboratory of Molecular Cardiovascular Sciences, Ministry of Education, Beijing, 100191, China

Abstract

Urea transporters (UT) are a family of transmembrane urea-selective channel proteins expressed in multiple tissues and play an important role in the urine concentrating mechanism of the mammalian kidney. UT inhibitors have been identified to have diuretic activity and might be developed as novel diuretics. To determine if functional deficiency of all UTs in all tissues causes

Address correspondence to: Baoxue Yang, M.D., Ph.D., Department of Pharmacology, School of Basic Medical Sciences, Peking University, 38 Xueyuan Lu, Haidian District, Beijing 100191, China, Phone: 86-10-82805622, baoxue@bjmu.edu.cn.
T. Jiang and Y. Li contributed equally to this work

DISCLOSURE
All the authors declare no conflict of interest.

physiological abnormality, we established a novel mouse model in which all UTs were knocked out by deleting an 87 kb of DNA fragment containing most parts of *Slc14a1* and *Slc14a2* genes. Western blot analysis and immunofluorescence confirmed that there is no expression of urea transporter in all-UT-knockout mice. Daily urine output was nearly 3.5-fold higher, with significantly lower urine osmolality, in all-UT-knockout-mice than that in wild-type mice, and urine osmolality was significantly lower. All-UT-knockout mice were not able to increase urinary urea concentration and osmolality after water deprivation, acute urea loading or high protein intake. A computational model that simulated UT knockout mouse models identified the individual contribution of each UT in urine concentrating mechanism. Knocking out all UTs also decreased the blood pressure and promoted the maturation of the male reproductive system. These results revealed that functional deficiency of all UTs caused urea selective urine concentrating defect with little physiological abnormality in extrarenal organs.

Keywords

urine concentration; renal physiology; gene targeting; knockout; animal model

INTRODUCTION

Urea, the end product of protein metabolism, plays an important role in the urine concentrating process and water conservation in the mammalian kidney.[1] Urea transporters (UT) are transmembrane urea-selective channel proteins that include two UT subfamilies, UT-A and UT-B, which are encoded by gene *Slc14a2* and *Slc14a1*, respectively.[2–10] UT-A subfamily includes six members, UT-A1 to UT-A6, which are derived from *Slc14a2* by two distinct promoters and splicing regulation.[11–13] UT-A1, the largest form in the subfamily, is expressed on the apical plasma membrane of the inner-medullary collecting duct (IMCD).[14, 15] UT-A2 shares the identical C-terminal part with UT-A1 and is expressed in the lower half of the thin descending limb of Henle's loops (TDL) in short-looped nephrons, and in the initial inner-medullary (IM) segments of the TDL in long-looped nephrons.[16] UT-A3 shares the same N-terminal as UT-A1 but stop codon in exon 13 (at the middle of *Slc14a2*) and is expressed in the IMCD basolateral plasma membrane.[17] UT-A4, which has the same N- and C-terminal amino acid sequences with UT-A1 and consists of the N-terminal quarter of UT-A1 spliced into the C-terminal quarter of UT-A1, is only detected in rat kidney medulla.[18] UT-A5 is expressed in mouse testis but not in kidney; its deduced amino acid sequence begins at methionine 139 of mouse UT-A3, after which it shares 100 % homology and a common C-terminus with mouse UT-A3.[19] UT-A6 is expressed in human colon but not in kidney.[20] UT-B has a wide distribution in the body, including erythrocytes, brain, spleen, heart, testis, bladder, and the endothelium of the vascular vessels and renal descending vasa recta (DVR).[11, 21–29]

The physiological functions of UTs have been revealed via the phenotypic analysis of several UT selective knockout mouse models.[30–38] The first UT knockout mouse model showed that UT-B functional deletion caused urea selective urea concentrating defect, resulting in a 25% decrease in urine osmolality and 50% increase in urine output.[5] These results highlight the role of UT-B in the countercurrent exchange of urea between ascending

and descending vasa recta. UT-A1/A3 double knockout mice exhibit strong urine concentrating defect, with a 70% reduction in urine osmolality. However, *in situ* transgenic expression of UT-A1 in UT-A1/A3 double knockout mice almost completely restores the urine concentrating effect, indicating that UT-A1 may play a major role in the urine concentrating mechanism of the mammalian kidney by facilitating the delivery of urea to the deep inner medulla.[30] UT-A2 deletion has only a minor effect on the urine concentration in mice with low protein diet. It is noteworthy that the urine concentrating ability of UT-B/UT-A2 knockout mice is partially restored, relative to UT-B knockout mice.[35] Taken together these experimental results suggest that UTs might be diuretic targets and that UT inhibitors might be developed as novel diuretics.[39]

By high-throughput screening using an erythrocyte lysis assay, several classes of small molecular UT inhibitors have been identified with IC_{50}s of submicromolar to micromolar.[40–42] The *in vitro* and *in vivo* experiments precluded proof-of-concept studies of their diuretic efficacy in rat and mouse models.[43, 44] Some UT inhibitors, such as thienoquinolins, inhibit both UT-B- and UT-A-type urea transporters. Subcutaneous delivery of thienoquinolin to rats caused an increase in urine output and a decrease in the urine urea concentration and osmolality, without causing electrolyte disturbance and liver or renal damage.[43] However, the physiological effect of UT inhibition in extrarenal systems remains to be better characterized.

To reveal any side effect of inhibitors of both UT-As and UT-B and to identify any physiological disorders when all organs lack UT, we generated a UT null (all-UT-knockout) mouse model by deleting a DNA fragment containing major parts of *Slc14a2* and *Slc14a1* genes. The phenotypic analysis shows that, with the exception of a more severe urea selective urine concentrating defect compared to other single or double UT knockout mice, UT null mice exhibit normal plasma urea and electrolyte concentration, low blood pressure and early maturation of the male reproductive system. These results suggest that UTs are effective diuretic targets and that UT inhibitors might be developed as potential diuretics without severe side effect.

RESULTS

Generation of all-UT-knockout mice

All-UT-knockout male mice were generated by the gene-targeting strategy shown in Fig. 1A. Western blot analysis revealed UT-A1 and UT-A3 in the inner medulla and both UT-B and UT-A2 in the outer medulla of the wild-type mice, but not in the all-UT-knockout mice (Fig. 1B). Urea and water permeabilities in erythrocytes were measured by stop-flow light scattering to detect the existence of UT-B. Urea permeability in the erythrocytes from all-UT-knockout mice was significantly lower than those from wild-type mice (Fig. 1C). UT-A and UT-B proteins were localized in mouse kidney tissue by immunofluorescence. Fig. 1D shows UT-A1 and UT-A3 expression in IMCD, UT-A2 expression in TDL and UT-B expression in DVR of wild-type kidneys (top). In contrast, there was no positive staining of UT-A1, UT-A2, UT-A3 and UT-B in all-UT-knockout mice (bottom). These experimental results confirmed that the *Slc14a2* and *Slc14a1* genes were successfully knocked out.

Genotype analysis of offspring from breeding of all-UT-knockout heterozygous mice indicated a nearly 1:2:1 fitting to the Mendelian distribution.

Urine concentrating ability in all-UT-knockout mice

An analysis of growth by mouse weight (age 1~8 weeks) showed no difference between wild-type and all-UT-knockout mice (Fig. 2A). Fig. 2B showed daily urinary output. The all-UT-knockout mice were severely polyuric, excreting almost 3-fold more fluid than litter-matched wild-type mice (Table 1). The average urine osmolality in all-UT-knockout mice was markedly lower than that in wild-type mice (Fig. 2C). Urinary concentrating ability was measured in response to a 24 h water deprivation. Urine osmolality increased substantially in the wild-type mice but only slightly in the all-UT-knockout mice. Histological examination showed dilatation of collecting ducts in the inner medulla in all-UT-knockout mice resulting from polyuria (Fig. 2D bottom). No other morphological abnormality was observed in the kidney cortex and outer medulla in both groups. The composition of the aqueous component of the inner medulla was shown in Fig. 2E. The inner medullary urea concentration in all-UT-knockout mice was significantly lower than that in wild-type mice. There was no obvious difference in sodium, potassium and chloride concentrations between two genotypes.

Osmolality and urea concentration were measured in urine and plasma under basal conditions. Urinary urea concentration was significantly lower in all-UT-knockout mice. However, plasma urea concentration was similar in the all-UT-knockout and wild-type mice. Plasma creatinine and creatinine clearance (an index of glomerular filtration rate) were similar in the two groups, suggesting that UT-As and UT-B deletion does not influence glomerular hemodynamics. The urine-to-plasma ration for urea, creatinine and electrolytes were severely lower in all-UT-knockout mice than in wild-type mice. There was no significant difference in sodium, potassium, and chloride concentrations in plasma between the two genotypes (Table 1).

Kidney weight (2 kidneys) was 347±29 and 344±43 mg in wild-type and all-UT-knockout mice, respectively. Kidney index was similar in two groups without influencing by both UT-A and UT-B deletion.

Urea excretion ability

To evaluate the contribution of all UT-As and UT-B in the capacity of kidney to excrete a load of urea, mice were subjected to an acute modest urea load (~1/10 of daily urea excretion). In the first 2 h after administration of urea load, all-UT-knockout mice increased their urine flow rate rapidly but showed only a small rise in urinary osmolality and urinary urea concentration, while wild-type mice significantly increased their urea concentration and urinary osmolality, with a modest rise in urinary flow rate (Fig. 3A–C). Interestingly, the time-course of urea excretion is similar in the two groups (Fig. 3D). After urea excretion returned to basal level (6~8 h after the load), urinary osmolality and urea concentration in wild-type mice remained elevated. In contrast, in all-UT-knockout mice, urinary osmolality was only modestly elevated and urine output declined slightly (268 μl/2h, 8 h after the load vs. 311 in basal period), indicating that mice could not accumulate urea in the medulla after

an acute urea load without UTs. Administration of exogenous urea significantly improved the ability of the kidney to concentrate other urinary solutes in wild-type mice, but this was not observed in all-UT-knockout mice (Fig. 3E). Because of the large urine output in the primary stage, the excretion of non-urea solutes was increased slightly in all-UT-knockout mice (Fig. 3F).

To evaluate the mechanisms by which mice of different genotypes chronically adapt their renal function to different levels of urea excretion, wild-type and all-UT-knockout mice were fed for 1 week with a diet containing 10, 20, or 40 percent protein. Protein intake had a significant influence on urine output, which increased in the two groups with the amount of diet protein. For a given protein content, urine flow rate was higher in all-UT-knockout mice than in wild-type mice (Fig. 4A). Urinary osmolality and urea concentration increased with the amount of diet protein in wild-type mice but changed only slightly in all-UT-knockout mice (Fig. 4B, C), suggesting that the long-term accumulation of urea in the inner medulla was disrupted without UTs. Osmolar excretion, urea excretion, and non-urea solutes excretion were similar in the two groups for each diet, as can be expected because of the similar food intake imposed on both groups (Fig. 4D–F).

Role of individual UT in urine concentrating mechanism predicted by mathematic modeling simulation

It is impossible to get the values of urine concentrating role played by each UT in physiological condition. Role of individual UT in urine concentrating mechanism was simulated basing on the data from wild-type and available UT knockout mouse models (Table 2), which include the present study and Refs[5, 30, 34, 35, 52]. Model parameters used in the rat simulations can be found in Ref[58]. Key predictions are summarized in Table 3.

To simulate UT-A2 knockout, urea permeability of the inner-stripe segment of the superficial descending limb and the upper inner-medullary segment of the juxtamedullary descending limb was reduced from the baseline value of 80×10^{-5} to 10^{-5} cm/s. The model predicted no significant impact on urine concentration and flow rate. To simulate UT-B knockout, plasma urea concentration was increased from 8 to 12 mmol/l, and DVR and red blood cell urea permeability was reduced by a factor of 45. UT-B knockout was predicted to impair urea cycling and substantially decrease the urea flow into the inner medulla via the DVR. In the inner medulla, where interstitial fluid exhibited an increasing urea concentration gradient, urea reabsorption from the DVR was reduced. Taken in isolation, that would augment the osmolality lag between the interstitial fluid and the DVR luminal fluid. Owing to the high DVR water permeability, more water was reabsorbed along the inner medullary DVR compared to base case.

In the wild-type model, urea permeability of the terminal IMCD was assumed to increase rapidly from 1×10^{-5} to 110×10^{-5} cm/s. To simulate UT-A1/3 knockout, IMCD urea permeability was assumed not to increase and to remain at 1×10^{-5} cm/s. As a result, urea reabsorption from the IMCD was substantially reduced: interstitial fluid urea concentration at the papillary decreased from its wild-type value of 560 mmol/l to 171 mmol/l. The IM urine concentrating mechanism was practically annihilated (compared CD fluid osmolality

at OM-IM boundary and urine osmolality). As in the case of UT-B knockout, deletion of UT-A3 or UT-A1/3 had little impact on the OM concentrating mechanism.

Finally, we simulated the all-UT-knockout model. We assumed that DVR and descending limb water permeability was not affected. With urea cycling from IMCD and DVR substantially impaired due to the deletion of UT-A1/3 and UT-B, respectively, the model predicted the lowest DVR urea flow into the IM (0.61 mmol/day, lower than the UT-B knockout value of 0.93), lowest papillary tip interstitial fluid urea concentration (113 mmol/l, lower than the UT-A1/3 knockout value of 172), and lowest urine osmolality (772 mosm/(kg H_2O)). Again, the impairment of the urine concentrating mechanism was restricted to the IM: deletion of all UTs had little impact on the OM concentrating mechanism.

The specificity of UT inhibitor PU-48

Because of the deficiency of all UTs, the all-UT-knockout mouse is the ideal model to assess the specificity of UT inhibitors that may be developed as diuretics. To verify our conjecture, 100 mg/kg PU-48 was subcutaneously injected to both wild-type and all-UT-knockout mice. After administration of PU-48, urine output in wild-type mice significantly increased, and urinary osmolality and urea concentration decreased, confirming the diuretic effect of PU-48 (Fig. 6). In contrast, PU-48 treatment produced no obvious change in urine output, urinary osmolality and urinary urea concentration in all-UT-knockout mice, indicating that PU-48 inhibited UTs specifically and did not affect other transporters that play a significant role in the urine concentrating mechanism. These results suggest that all-UT-knockout mice may be used as a model to assess the specificity of UT inhibitors.

Extrarenal phenotypes of all-UT-knockout mice

We seek to determine whether all-UT-knockout mice exhibit depression-like behavior found in UT-B null mice.[45] Forced swim test and sucrose preference test were performed as previously described.[45] The period of immobility in forced swim test was used to characterize depression-like behavior. The time of immobility obtained for the all-UT-knockout and wild-type mice was similar (84±11 s *vs.* 87±13 s; Fig. 7A left). The preferential consumption of sucrose solution was performed to check the loss of appetitive motivation. Sucrose preference showed no significant difference between the two genotypes (Fig. 7A right). These results suggest that UTs deletion did not cause depression-like behavior, which may be attributable to elevation in plasma urea concentration.

Blood pressure was measured using a computerized tail cuff system with a photoelectric sensor.[46] Diastolic blood pressure (DBP; 103±6 *vs.* 110±5, 98±8 mmHg, $p<0.05$), systolic blood pressure (SBP, 134±6 *vs.* 142±6, 130±7mmHg, $p<0.05$) and mean arterial pressure (MAP, 114±8 *vs.*121±7, 110±8 mmHg, $p<0.05$) were all lower in all-UT-knockout mice than those in wild-type mice, but higher than those in UT-B null mice (Fig. 7B).

To determine the effect of UTs deletion on the development of the male reproductive system, we examined appearance time of sperm in testes. At 24 days of age, elongating spermatids appeared in all-UT-knockout male mice, but none was present in wild-type males until day 32 (Fig. 7C). The data indicate an early attainment of sexual maturity in all-UT-knockout

mice. The competing mate experiments showed that the time to the first litter in the competing mate groups (69±2.5 days) was significantly earlier than the control groups (78.2±2.4 days), indicating that the breeding ages were 48±2.5 days in the competing mating groups and 57.2±2.4 days in the control (Fig. 7D). The genotypes of all pups in the competing mate groups were all-UT-knockout heterozygotes, which indicates that all pups in competing mate groups carried the targeted all-UT-knockout gene and were produced by all-UT-knockout male mice. The numbers and gender ratios of pups sired by all-UT-knockout mice in competing mate groups were similar to those produced by wild-type males in the control groups.

DISCUSSION

UT-As and UT-B are homologues and are expressed in various tissues and cell types.[6, 47] Many UT inhibitors (e.g., PU-48) are known to inhibit all UTs. Thus, it is crucial to determine whether there were severe physiological disorders without any UT in the body. Another goal of this study was to determine the contribution of each UT to intrarenal urea recycling and to the urine concentration mechanism of the mammalian kidney. That goal was accomplished by comparing data derived from all-UT-knockout mice with UT-A2, UT-A3, UT-A1/A3, UT-A2/B and UT-B null mice. A third goal of was to establish an all-UT-knockout mouse model to determine the specificity of novel UT inhibitors.

To knockout all UTs simultaneously is a challenging task. The UT-A and UT-B genes, *Slc14a2* and *Slc14a1*, respectively, are linked in a huge DNA fragment of approximately 330 kb in length.[48–50] The *Slc14a2* gene, a very large gene including 24 exons, is approximately 300 kb in length,[49] whereas the *Slc14a1* gene, which includes 11 exons, is approximately 30 kb in length.[51] To delete all functional UT proteins, we designed a gene targeting strategy to knock out an 87-kb-long gene region covering exon 4 to exon 24 of the *Slc14a2* gene, including coding region of all UT-As, and exon 1 to exon 7 of the *Slc14a1* gene, including most part of coding region of UT-B. Indeed, to the best of our knowledge, that is the longest knockout fragment using common gene targeting technology. Using this strategy, whole family of UTs were knocked out by a gene targeting. A mouse model with all UTs deletion was successfully generated, and validated by means of UTs expression detection and functional analysis.

Experimental results showed that all-UT-knockout mice exhibited grossly normal phenotype, except low urine concentrating ability, slightly lower blood pressure and early maturation of the male reproductive system. No change was found in either plasma creatinine or creatinine clearance of all-UT-knockout mice, demonstrating that UTs deletion did not influence normal glomerular filtration rate. Interestingly, plasma Na^+, K^+, and Cl^- concentrations were similar between two genotypes, indicating that the deletion of all UTs increased urine output without electrolyte disturbance (Table 1). There appeared to be no morphological change in cortex and outer medulla of all-UT-knockout mice, except collecting duct dilatation due to large urine output.

All-UT-knockout mice showed a larger urine output than all the other UT knockout mice. The reason is that less urea was reabsorbed at the end of IMCD and less urea was returned to

the inner medulla by DVR (by UT-B), which led to a lower urea concentration in inner medulla of all-UT-knockout mice than wild-type mice. Compared with wild-type mice, neither an acute nor a chronic urea load increased urinary urea concentration and osmolality, indicating all-UT-knockout could not accumulate urea in the inner medulla.

With the addition of the new all-UT-knockout model, there are currently six models of UT knockout mice, including UT-B single knockout,[5] UT-A1/A3 double knockout,[30] UT-A2 single knockout,[34] UT-A2/B double knockout,[35] and UT-A1/A3 double knockout with UT-A1 rescue.[52] All these mice were alive at adult age and their phenotypes have been analyzed to determine the physiological functions of each UT. Urine concentrating ability has been the primary focus in these UT knockout mouse models. The degree of urine concentrating deficiency among these mice: all-UT-knockout mice > UT-A1/A3 null mice > UT-B null mice > UT-A2/B null mice > UT-A3 null mice > UT-A2 null mice (Table 2). Osmolality in inner medullary tissue: all-UT-knockout mice < UT-A1/A3 null mice < UT-B null mice < UT-A2/B null mice < wild-type mice. High blood urea concentration was found only in UT-B null mice. Other mice with single or double UTs deletion have normal or lower blood urea concentration. These data suggest UT-A1 is the most important UT in intrarenal urea recycling and urine concentrating mechanism. UT-B is essential in intrarenal urea recycling and in maintaining a normal blood urea level. No clear role in the urine concentrating mechanism has been identified for UT-A2 and UT-A3.

Mathematical model simulations suggest that the impact of any UT deletion on the urine concentrating mechanism is restricted to the IM. The outer-medullary concentrating mechanism is driven principally by the active Na^+ reabsorption along the thick ascending limbs of the loops of Henle and does not depend on urea. Thus, the concentrating capacity of the outer medulla, as measured by the collecting duct luminal fluid osmolality at the inner-outer medullary boundary, is little affected in any of the UT deletion simulations. There is a discrepancy between the measured data and simulation, which may be attributed, in part, to the major difference between the computational model and the experimental knockout studies. Morphological and transport parameters used in the computational model are based on measurements in the rat kidney, whereas the knockout studies were conducted in the mice. Thus, while model simulation results can provide insights, they may not be directly comparable to the experimental data. In fact, mice have a significantly higher urea excretion rate and highly daily load of urea per gram of kidney weight compared to rat.[53] Consequently, impaired urea trapping may have a larger impact on the urine concentrating mechanism of a mouse kidney than that of a rat (or, a computational model of a rat kidney).

Besides the kidney, UT-B is widely distributed in many tissues such as the brain, heart, liver and testis. To explore the effect of all UTs deletion on extrarenal organs, we measured urea concentration in different organs of all-UT-knockout mice. Urea concentration in the brain did not change after UT-As and UT-B deletion. Forced swim test and sucrose preference test also confirmed that all-UT-knockout mice had no depression-like behavior. That result that differs findings in UT-B null mice,[45] where in UT-B deletion elevated urea concentration that decreased NO production in hippocampus, then caused depression-like behavior. Plasma and brain urea concentrations were at normal levels in all-UT-knockout mice, confirming

that the depression-like behavior was attributable to elevated urea concentration level rather than directly to the deletion of UT proteins.

Our previous results showed that UT-B deletion caused low blood pressure. A possible mechanism is that the intracellular urea accumulation in endothelial cells decreases the arginase expression and activity, which then increases eNOS expression and activity and induces NO-mediated endothelium-dependent vascular relaxations.[46] However, we could not eliminate the possibility of an anti-hypertensive effect through diuresis in UT-B null mice. Results in the present study indicated that blood pressure in all-UT-knockout mice was lower than wild-type mice but higher than UT-B null mice. We speculated that the low blood pressure in all-UT-knockout mice was caused by diuresis. These results hinted that UT-B inhibitors lowered blood pressure by both diuresis and high NO production, and could become a novel strategy for the treatment of hypertension.

Guo et al. reported that UT-B deletion promoted the maturation of the male reproductive system.[54] The coincident phenomenon was observed in all-UT-knockout mice. The urea concentration in all-UT-knockout testis was higher than wild-type mice and similar to UT-B null mice. Taken together, our findings confirmed that it was the accumulation of urea in the testis rather than urea in plasma that caused early maturation of the male reproductive system.

Thienoquinolin UT inhibitors, which inhibit both UT-B and UT-As, have been considered as new diuretic drug candidates.[43, 44] However, it remains to be determined whether these compounds inhibit only UTs. After administration of PU-48 (a Thienoquinolin UT inhibitor), urine volume did not increase in all-UT knockout mice, which confirms the specificity of PU-48 in inhibiting UTs. Therefore, all-UT-knockout mouse is an ideal animal model to assess the specificity of novel UT inhibitors.

METHODS

Generation of all-UT-knockout mice

A targeting vector for homologous recombination was constructed with a 5-kb genomic UT-B DNA fragment (left arm) and a 3-kb fragment (right arm). The left and right arm genomic fragments were PCR-amplified, and a DTA cassette was inserted upstream for negative selection. The targeting vector was linearized at a unique downstream NotI site and electroporated into C57BL/6 embryonic stem cells. Transfected embryonic stem cells were selected with G418, yielding 12 targeted clones from 1167 doubly resistant colonies on PCR screening with a neo-specific sense primer for a 3.36 kb fragment. Homologous recombination was confirmed by Southern blot analysis. Embryonic stem cells were injected into post coitus 2.5-day eight-cell morula stage CD1 zygotes, cultured overnight to blastocysts, and transferred to pseudopregnant C57 females. Offspring were genotyped by PCR followed by Southern blot analysis as described above. Heterozygous founder mice containing the disrupted *Slc14a2* and *Slc14a1* genes in the germ line were bred to produce homozygous All-UT-knockout mice. Protocols were approved by the Peking University Health Center Committee on Animal Research.

Western blot analysis

Kidney tissues were homogenized in RIPA lysis buffer containing protease inhibitor cocktail (Roche, 11873580001). Total protein was assayed using BCA (Pierce Biotechnology, Rockford, IL, USA) and the size was separated by sodium dodecyl sulfate–polyacrylamide gel electrophoresis. Proteins were blotted to polyvinylidene difluoride membranes (Amersham Biosciences, Piscataway, NJ, USA). Blots were incubated with antibodies against UT-A2, UT-A3 and UT-B. Goat anti-rabbit IgG was added and the blots were developed with ECL plus kit (Amersham Biosciences).

Immunofluorescence and HE staining

Kidney was dissected out and fixed overnight in the 4% paraformaldehyde. The specimens were transferred to a solution containing 30% sucrose in 0.1 M phosphate buffer, pH 7.4. Kidney was cut at 7 μm on a cryostat. The sections were blocked with 10% normal goat serum containing 1% (w/v) bovine serum albumin, 0.1% Triton X-100, and 0.05% Tween-20 overnight at 4°C to avoid unspecific staining. Then, the sections were incubated with polyclonal antibodies against UT-A2, UT-A3 (home made) and anti-UT-B (a kindly gift from Dr. Trinh-Trang-Tan, INSERM, Paris, France). The secondary antibodies (Cy3-Goatanti-Rabbit, 1:200, Jackson ImmunoResearch Inc., USA) were added and incubated for 0.5 h, then placed in a solution containing Hoechst (1:1000, Leagene, Beijing, China) for 1 minute to stain nuclei. The images were captured by Leica fluorescence microscope (Germany). Heart, liver, spleen, kidney, bladder, and testis were obtained and fixed in 4% formaldehyde for paraffin embedding. Paraffin-embedded tissues were sectioned at 7 μm for hematoxylin and eosin staining.

Erythrocyte urea and water permeability measurements

Fresh erythrocytes obtained by tail bleeding (100~200 μl/bleed) were washed three times in phosphate-buffered saline to remove plasma and the cellular buffy coat. Stopped-flow measurements were carried out on a Hi-Tech Sf-51 instrument. For measurement of osmotic water permeability, suspensions of erythrocytes (~0.5% hematocrit) in phosphate-buffered saline were subjected to a 250 mM inwardly directed gradient of sucrose. The kinetics of decreasing cell volume was measured from the time course of 90° scattered light intensity at 530 nm wavelength. Osmotic water permeability coefficients (P_f) were computed from the light scattering time course.[55] For the measurement of urea permeability, the erythrocyte suspension was subjected to a 250 mM inwardly directed gradient of urea.

Urine concentrating studies

Adult male wild-type and all-UT-knockout mice (6 mice/group, body weight 22~25 g) were placed in metabolic cages adapted for mice (Harvard Apparatus, Holliston, MA). After two days of adaptation to the cages, urine samples were collected for 24 h under paraffin oil (to prevent evaporation). In some experiments, urine samples were obtained from the same mice under basal conditions (unrestricted access to food and water), and after 24-h deprivation of food and water. Twenty-four-hour urine output and water consumption were measured with metabolic cages. Blood samples were collected in heparinized glass tubes by puncture of the periorbital venous sinus. Plasma was separated from blood cells by centrifugation. Urine

osmolality was measured by freezing point osmometry (micro-osmometer, Precision Systems, Natick, MA). Urine and plasma chemistries were measured by the Peking University Third Hospital Clinical Chemistry Laboratory.

Acute urea load

Adult male wild-type and all-UT-knockout mice (6 mice/group, body weight 22~25 g) were adapted for 2 days before the urea load experiment to metabolic cages. Three hundred μl of 1M urea solution was administered by intraperitoneal injection. Urine was collected in 2-h fractions for 2 h before and 10 h after the urea load, and analyzed as described previously. Non-urea solute concentration was calculated by substracting urea concentration from urine.

Chronic alteration in protein intake

Adult male wild-type and all-UT-knockout mice (6 mice/group, body weight 22~25 g) were offered synthetic food (AIN 93G Bioserv) with either low (LP)-, normal (NP)-, or high (HP)-protein content (10, 20, or 40% casein, respectively, as the only source of protein). After 7 days on these diets, 24 h urine was collected and analyzed as described previously.[53]

Forced swim test

The forced swim test was applied as described by Porsolt.[56] Mice were placed individually into glass cylinders (height, 25 cm; diameter, 20 cm) containing water maintained at 23~25°C at a depth of 15 cm. Animals were tested for 6 min. The time of immobility was assessed during the last 5 min (after 1 min of habituation). A mouse was judged to be immobile when it remained floating in an upright position, making only small movements to keep its head above water.

Sucrose preference test

On the first day, two 1% sucrose droppers were placed in each cage to familiarize the mice with sucrose. On the second day, two droppers, one containing 1% sucrose and the other containing water, were placed in each cage. To avoid potential side preferences, the position of the droppers was switched on the third day and the fourth day. The consumption of water and sucrose solution was assessed on the fourth day. The preference for sucrose was calculated as the volume of sucrose solution consumed relative to the total volume of liquid consumed.[57]

Blood pressure measurement

Blood pressure was measured using a computerized tail cuff system (Hatteras Instruments, Cary, NC) with a photoelectric sensor. Blood pressure was recorded daily at 8:30 a.m. and averaged over five consecutive recordings.

Mating studies

A 28-day-old all-UT-knockout male mouse and a wild-type male mouse from the same litter were mated with a 64-day-old wild-type female. Two wild-type males were mated with a wild-type female in each control group. Animals were maintained under well-controlled conditions of temperature (22 °C), light, and humidity with food and water provided ad

libitum. The age of male mice was recorded when the first litter was delivered in each group. Breeding ages of male mice were deduced by deducting 21 days from the ages at delivery time. The size of the litter and gender of pups was recorded.

Computational modeling

A published computational model of water and solute transport in the renal medulla of the rat kidney[58] was used to assess the contributions of individual urea transporter. The model is formulated for steady state and represents loops of Henle, collecting ducts, and vasa recta. Model simulations predicted luminal flows and transmural fluxes of water, NaCl, and urea, as well as interstitial fluid and luminal fluid NaCl and urea concentrations at differing medullary levels. The transmural permeabilities of tubular and vascular segments to water and solutes were chosen based on anatomic, microperfusion, and immunochemistry data. We simulated the effects of deleting specific urea transport or transporters by changing the urea permeability of appropriate tubular or vascular segments.

Statistics

Data are expressed as mean ± SEM. All experiments were repeated at least 3 times (≧3 replicates) on each specimen and there were 3 specimens from each group. The results of all replicates from each specimen were averaged, and the mean of averaged values from all specimens of a single group was regarded as the corresponding value of the whole group. Data thus obtained from each group were tested by one-way ANOVA and, whenever needed, post-hoc LSD test to detect any between-group differences. A p value < 0.05 was considered statistically significant.

Acknowledgments

This work was supported by National Natural Science Foundation of China grants 31200869, 81261160507, 81330074 and 81170632, the Research Fund for the Doctoral Program of Higher Education 20100001110047, the 111 Project, International Science & Technology Cooperation Program of China grant 2012DFA11070 to Yang, and the National Institutes of Health (National Institute of Diabetes and Digest and Kidney Disease) via grants DK089066 and DK106102 to Layton.

References

1. Fenton RA, Chou CL, Sowersby H, et al. Gamble's "economy of water" revisited: studies in urea transporter knockout mice. Am J Physiol Renal Physiol. 2006; 291(1):F148–F154. [PubMed: 16478978]
2. Fenton RA. Urea transporters and renal function: lessons from knockout mice. Curr Opin Nephrol Hypertens. 2008; 17(5):513–518. [PubMed: 18695393]
3. Shayakul C, Hediger MA. The SLC14 gene family of urea transporters. Pflugers Arch. 2004; 447(5):603–609. [PubMed: 12856182]
4. Stewart G. The emerging physiological roles of the SLC14A family of urea transporters. Br J Pharmacol. 2011; 164(7):1780–1792. [PubMed: 21449978]
5. Yang B, Bankir L, Gillespie A, et al. Urea-selective concentrating defect in transgenic mice lacking urea transporter UT-B. J Biol Chem. 2002; 277(12):10633–10637. [PubMed: 11792714]
6. Sands JM, Timmer RT, Gunn RB. Urea transporters in kidney and erythrocytes. Am J Physiol. 1997; 273(3 Pt 2):F321–F339. [PubMed: 9321905]
7. Sands JM, Blount MA. Genes and proteins of urea transporters. Subcell Biochem. 2014; 73:45–63. [PubMed: 25298338]

8. Levin EJ, Zhou M. Structure of urea transporters. Subcell Biochem. 2014; 73:65–78. [PubMed: 25298339]
9. Ran J, Wang H, Hu T. Clinical aspects of urea transporters. Subcell Biochem. 2014; 73:179–191. [PubMed: 25298346]
10. Bankir L. Active urea transport in lower vertebrates and mammals. Subcell Biochem. 2014; 73:193–226. [PubMed: 25298347]
11. Timmer RT, Klein JD, Bagnasco SM, et al. Localization of the urea transporter UT-B protein in human and rat erythrocytes and tissues. Am J Physiol Cell Physiol. 2001; 281(4):C1318–C1325. [PubMed: 11546670]
12. Bagnasco SM. Gene structure of urea transporters. Am J Physiol Renal Physiol. 2003; 284(1):F3–F10. [PubMed: 12473534]
13. Klein JD. Expression of urea transporters and their regulation. Subcell Biochem. 2014; 73:79–107. [PubMed: 25298340]
14. Nielsen S, Digiovanni SR, Christensen EI, et al. Cellular and subcellular immunolocalization of vasopressin-regulated water channel in rat kidney. Proc Natl Acad Sci U S A. 1993; 90(24):11663–11667. [PubMed: 8265605]
15. Sands JM. Regulation of renal urea transporters. J Am Soc Nephrol. 1999; 10(3):635–646. [PubMed: 10073615]
16. Sands JM. Urea Transport: It's Not Just "Freely Diffusible" Anymore. News Physiol Sci. 1999; 14:46–47. [PubMed: 11390818]
17. Blount MA, Klein JD, Martin CF, et al. Forskolin stimulates phosphorylation and membrane accumulation of UT-A3. Am J Physiol Renal Physiol. 2007; 293(4):F1308–F1313. [PubMed: 17686955]
18. Karakashian A, Timmer RT, Klein JD, et al. Cloning and characterization of two new isoforms of the rat kidney urea transporter: UT-A3 and UT-A4. J Am Soc Nephrol. 1999; 10(2):230–237. [PubMed: 10215321]
19. Fenton RA, Howorth A, Cooper GJ, et al. Molecular characterization of a novel UT-A urea transporter isoform (UT-A5) in testis. Am J Physiol Cell Physiol. 2000; 279(5):C1425–C1431. [PubMed: 11029290]
20. Smith CP, Potter EA, Fenton RA, et al. Characterization of a human colonic cDNA encoding a structurally novel urea transporter, hUT-A6. Am J Physiol Cell Physiol. 2004; 287(4):C1087–C1093. [PubMed: 15189812]
21. Trinh-Trang-Tan MM, Cartron JP, Bankir L. Molecular basis for the dialysis disequilibrium syndrome: altered aquaporin and urea transporter expression in the brain. Nephrol Dial Transplant. 2005; 20(9):1984–1988. [PubMed: 15985519]
22. Hall GD, Smith B, Weeks RJ, et al. Novel urothelium specific gene expression identified by differential display reverse transcriptase-polymerase chain reaction. J Urol. 2006; 175(1):337–342. [PubMed: 16406938]
23. Inoue H, Kozlowski SD, Klein JD, et al. Regulated expression of renal and intestinal UT-B urea transporter in response to varying urea load. Am J Physiol Renal Physiol. 2005; 289(2):F451–F458. [PubMed: 15798087]
24. Berger UV, Tsukaguchi H, Hediger MA. Distribution of mRNA for the facilitated urea transporter UT3 in the rat nervous system. Anat Embryol (Berl). 1998; 197(5):405–414. [PubMed: 9623675]
25. Collins D, Winter DC, Hogan AM, et al. Differential protein abundance and function of UT-B urea transporters in human colon. Am J Physiol Gastrointest Liver Physiol. 2010; 298(3):G345–G351. [PubMed: 19926813]
26. Doran JJ, Klein JD, Kim YH, et al. Tissue distribution of UT-A and UT-B mRNA and protein in rat. Am J Physiol Regul Integr Comp Physiol. 2006; 290(5):R1446–R1459. [PubMed: 16373440]
27. Olives B, Martial S, Mattei MG, et al. Molecular characterization of a new urea transporter in the human kidney. FEBS Lett. 1996; 386(2–3):156–160. [PubMed: 8647271]
28. Olives B, Neau P, Bailly P, et al. Cloning and functional expression of a urea transporter from human bone marrow cells. J Biol Chem. 1994; 269(50):31649–31652. [PubMed: 7989337]
29. Yang B. Transport characteristics of urea transporter-B. Subcell Biochem. 2014; 73:127–135. [PubMed: 25298342]

30. Fenton RA, Chou CL, Stewart GS, et al. Urinary concentrating defect in mice with selective deletion of phloretin-sensitive urea transporters in the renal collecting duct. Proc Natl Acad Sci U S A. 2004; 101(19):7469–7474. [PubMed: 15123796]
31. Fenton RA, Knepper MA. Urea and renal function in the 21st century: insights from knockout mice. J Am Soc Nephrol. 2007; 18(3):679–688. [PubMed: 17251384]
32. Fenton RA, Flynn A, Shodeinde A, et al. Renal phenotype of UT-A urea transporter knockout mice. J Am Soc Nephrol. 2005; 16(6):1583–1592. [PubMed: 15829709]
33. Sands JM. Mammalian urea transporters. Annu Rev Physiol. 2003; 65:543–566. [PubMed: 12524463]
34. Uchida S, Sohara E, Rai T, et al. Impaired urea accumulation in the inner medulla of mice lacking the urea transporter UT-A2. Mol Cell Biol. 2005; 25(16):7357–7363. [PubMed: 16055743]
35. Lei T, Zhou L, Layton AT, et al. Role of thin descending limb urea transport in renal urea handling and the urine concentrating mechanism. Am J Physiol Renal Physiol. 2011; 301(6):F1251–F1259. [PubMed: 21849488]
36. Sands JM. Molecular approaches to urea transporters. J Am Soc Nephrol. 2002; 13(11):2795–2806. [PubMed: 12397052]
37. Chen G. Biochemical properties of urea transporters. Subcell Biochem. 2014; 73:109–126. [PubMed: 25298341]
38. Fenton RA, Yang B. Urea transporter knockout mice and their renal phenotypes. Subcell Biochem. 2014; 73:137–152. [PubMed: 25298343]
39. Yang B, Bankir L. Urea and urine concentrating ability: new insights from studies in mice. Am J Physiol Renal Physiol. 2005; 288(5):F881–F896. [PubMed: 15821253]
40. Esteva-Font C, Phuan PW, Anderson MO, et al. A small molecule screen identifies selective inhibitors of urea transporter UT-A. Chem Biol. 2013; 20(10):1235–1244. [PubMed: 24055006]
41. Yang B, Verkman AS. Analysis of double knockout mice lacking aquaporin-1 and urea transporter UT-B. Evidence for UT-B-facilitated water transport in erythrocytes. J Biol Chem. 2002; 277(39):36782–36786. [PubMed: 12133842]
42. Verkman AS, Esteva-Font C, Cil O, et al. Small-molecule inhibitors of urea transporters. Subcell Biochem. 2014; 73:165–177. [PubMed: 25298345]
43. Li F, Lei T, Zhu J, et al. A novel small-molecule thienoquinolin urea transporter inhibitor acts as a potential diuretic. Kidney Int. 2013; 83(6):1076–1086. [PubMed: 23486518]
44. Ren H, Wang Y, Xing Y, et al. Thienoquinolins exert diuresis by strongly inhibiting UT-A urea transporters. Am J Physiol Renal Physiol. 2014; 307(12):F1363–F1372. [PubMed: 25298523]
45. Li X, Ran J, Zhou H, et al. Mice lacking urea transporter UT-B display depression-like behavior. J Mol Neurosci. 2012; 46(2):362–372. [PubMed: 21750947]
46. Sun Y, Lau CW, Jia Y, et al. Functional inhibition of urea transporter UT-B enhances endothelial-dependent vasodilatation and lowers blood pressure via L-arginine-endothelial nitric oxide synthase-nitric oxide pathway. Sci Rep. 2016; 6:18697. [PubMed: 26739766]
47. Sands JM, Layton HE. Advances in understanding the urine-concentrating mechanism. Annu Rev Physiol. 2014; 76:387–409. [PubMed: 24245944]
48. Artagaveytia N, Elalouf JM, de Rouffignac C, et al. Expression of urea transporter (UT-A) mRNA in papilla and pelvic epithelium of kidney in normal and low protein fed sheep. Comp Biochem Physiol B Biochem Mol Biol. 2005; 140(2):279–285. [PubMed: 15649775]
49. Nakayama Y, Naruse M, Karakashian A, et al. Cloning of the rat Slc14a2 gene and genomic organization of the UT-A urea transporter. Biochim Biophys Acta. 2001; 1518(1–2):19–26. [PubMed: 11267655]
50. Promeneur D, Rousselet G, Bankir L, et al. Evidence for distinct vascular and tubular urea transporters in the rat kidney. J Am Soc Nephrol. 1996; 7(6):852–860. [PubMed: 8793793]
51. Lucien N, Sidoux-Walter F, Olives B, et al. Characterization of the gene encoding the human Kidd blood group/urea transporter protein. Evidence for splice site mutations in Jknull individuals. J Biol Chem. 1998; 273(21):12973–12980. [PubMed: 9582331]
52. Klein JD, Wang Y, Mistry A, et al. Transgenic Restoration of Urea Transporter A1 Confers Maximal Urinary Concentration in the Absence of Urea Transporter A3. J Am Soc Nephrol. 2015

53. Bankir L, Chen K, Yang B. Lack of UT-B in vasa recta and red blood cells prevents urea-induced improvement of urinary concentrating ability. Am J Physiol Renal Physiol. 2004; 286(1):F144–F151. [PubMed: 12965892]

54. Guo L, Zhao D, Song Y, et al. Reduced urea flux across the blood-testis barrier and early maturation in the male reproductive system in UT-B-null mice. Am J Physiol Cell Physiol. 2007; 293(1):C305–C312. [PubMed: 17475664]

55. Yang B, Ma T, Verkman AS. Erythrocyte water permeability and renal function in double knockout mice lacking aquaporin-1 and aquaporin-3. J Biol Chem. 2001; 276(1):624–628. [PubMed: 11035042]

56. Porsolt RD, Le Pichon M, Jalfre M. Depression: a new animal model sensitive to antidepressant treatments. Nature. 1977; 266(5604):730–732. [PubMed: 559941]

57. Popa D, Lena C, Alexandre C, et al. Lasting syndrome of depression produced by reduction in serotonin uptake during postnatal development: evidence from sleep, stress, and behavior. J Neurosci. 2008; 28(14):3546–3554. [PubMed: 18385313]

58. Moss R, Layton AT. Dominant factors that govern pressure natriuresis in diuresis and antidiuresis: a mathematical model. Am J Physiol Renal Physiol. 2014; 306(9):F952–F969. [PubMed: 24553433]

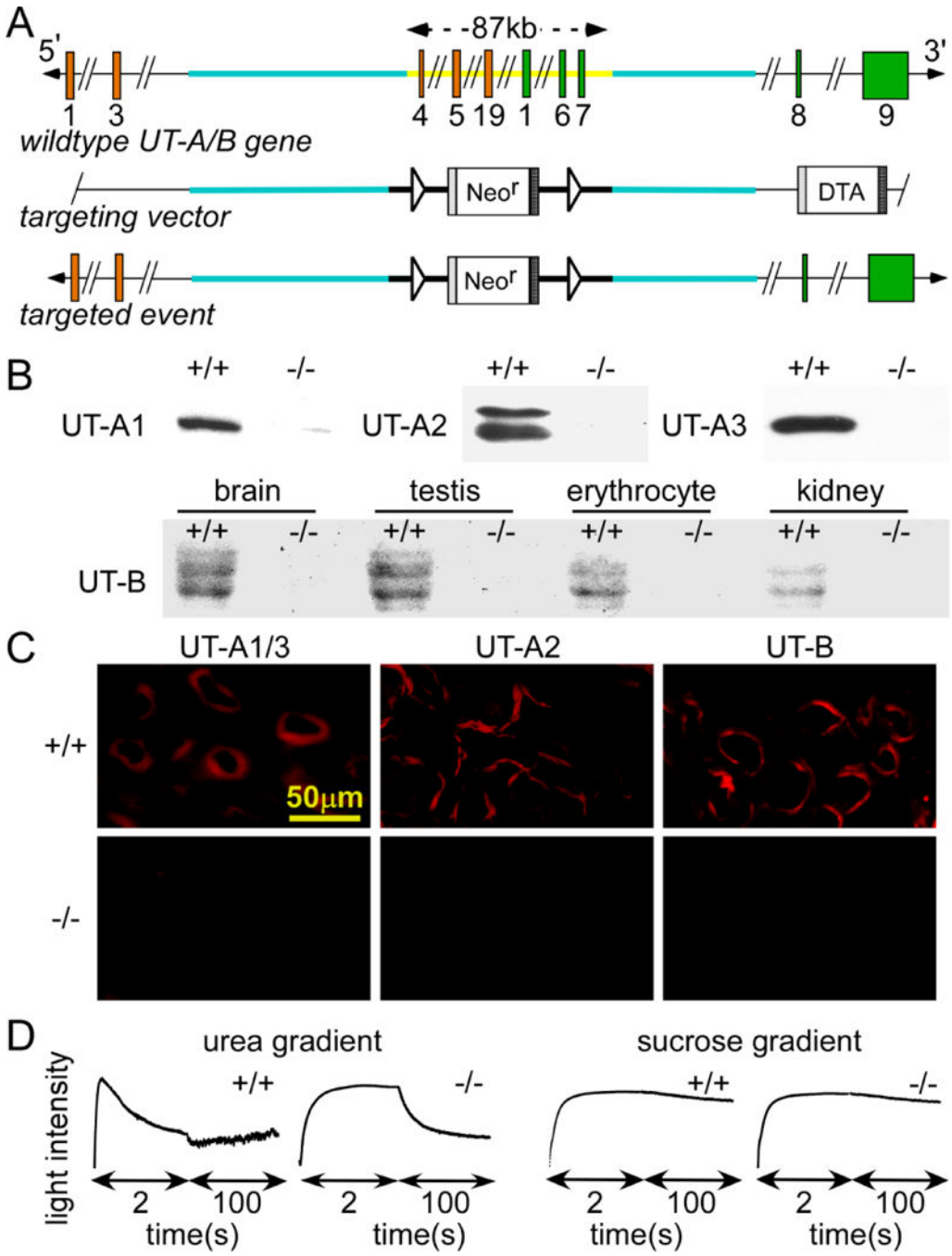

Fig. 1. Gene targeting strategy for all-UT-knockout and identification of all-UT-knockout mice

A. *top*, organization and restriction map of the mouse *Slc14a2* and *Slc14a1* genes. Rectangles indicate exon segments that constitute coding sequences. *Middle* and *bottom*, targeting strategy for all UTs deletion. Homologous recombination results in the replacement of the indicated segments (thick line) of the *Slc14a2* and *Slc14a1* genes by a neo cassette selectable marker flanked by LoxP sites. DTA is used for negative selection. The constitutive knockout allele was obtained after Cre-mediated recombination. **B.** Western blot analysis of kidney using UT-A2, UT-A3 or UT-B antibody. **C.** UT-A1/A3, UT-A2 and

UT-B immunofluorescence of kidney inner and outer medulla stained by UT-A3, UT-A2 or UT-B antibody. **D.** urea permeability measured in erythrocytes from wild-type and all-UT-knockout mice from the time course of erythrocyte volume as determined by light scattering in response to a 250 mM inwardly directed urea gradient (*left*). Water permeability measured in response to a 250 mM inwardly directed sucrose gradient (*right*, n=3).

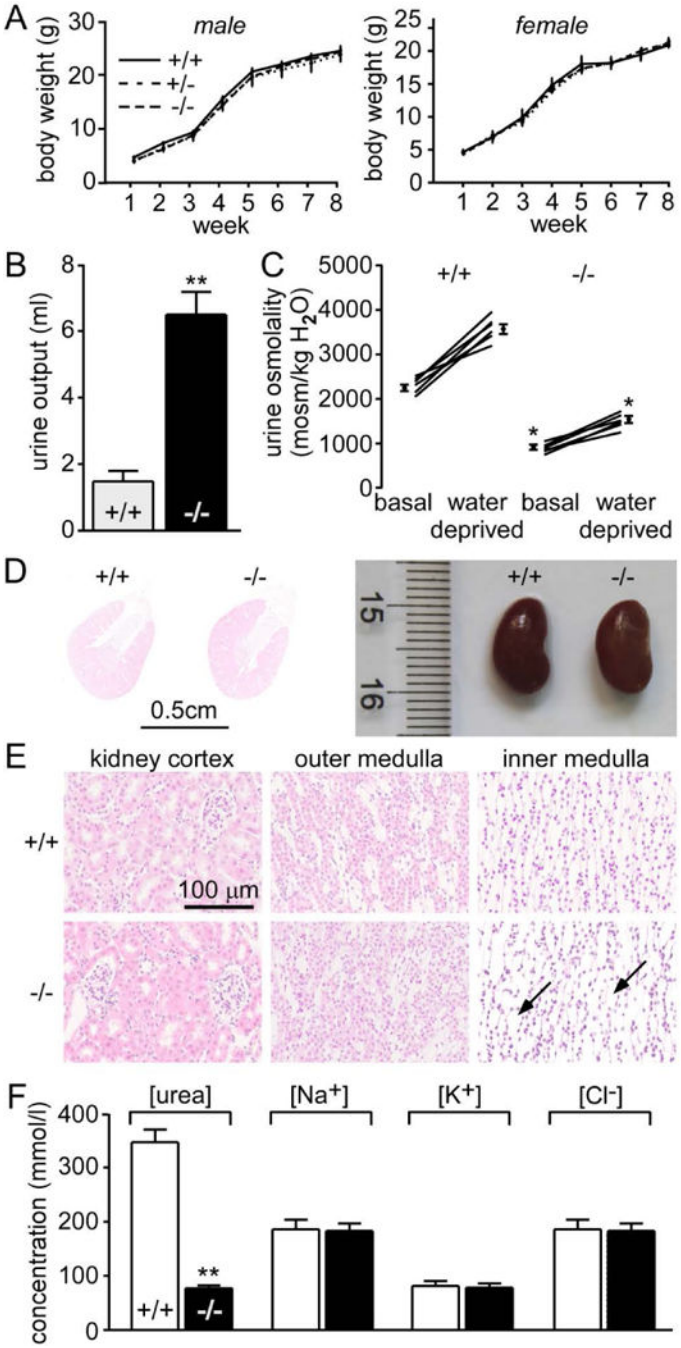

Fig. 2. Renal phenotype of all-UT-knockout mice

A. body weight. **B.** 24 h urine output. **C.** urine osmolality measured in mice given free access to food and water (basal) and after a 24 h water deprivation. Means ± SEM, n = 6. **D.** representative images of H&E staining of kidney cortex, outer medulla and inner medulla of wild-type mice (*upper*) and all-UT-knockout mice (*lower*). Scale bar =100µm. **E.** urea concentration, sodium concentration, potassium concentration, and chloride concentration in inner medullary tissue. Data are presented as means ± SEM. n=6. **p < 0.01; *p < 0.05 *vs.* wild-type mice.

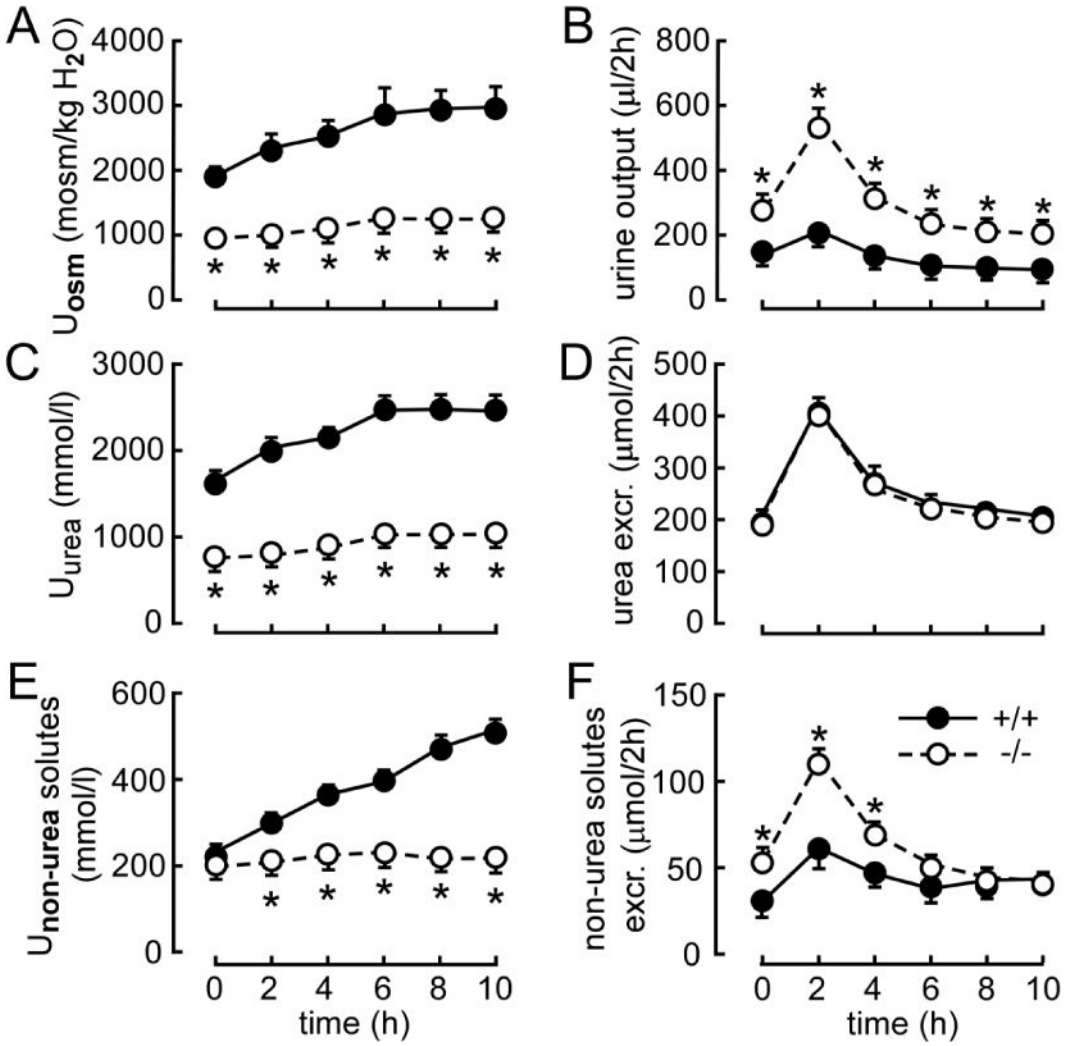

Fig. 3. Renal handling of acute urea loading

Three hundred micromoles of urea were injected (*ip*) just after the first 2-h urine collection (time 0). **A.** urinary osmolality (U_{osm}). **B.** urinary output. **C.** urinary urea concentration (U_{urea}). **D.** urea excretion (excr.). **E.** nonurea solute concentration ($U_{non\text{-}urea\ solutes}$). **F.** excretion of non-urea solutes. Data are presented as means ± SEM. n = 6. *p < 0.05 *vs.* wild-type mice.

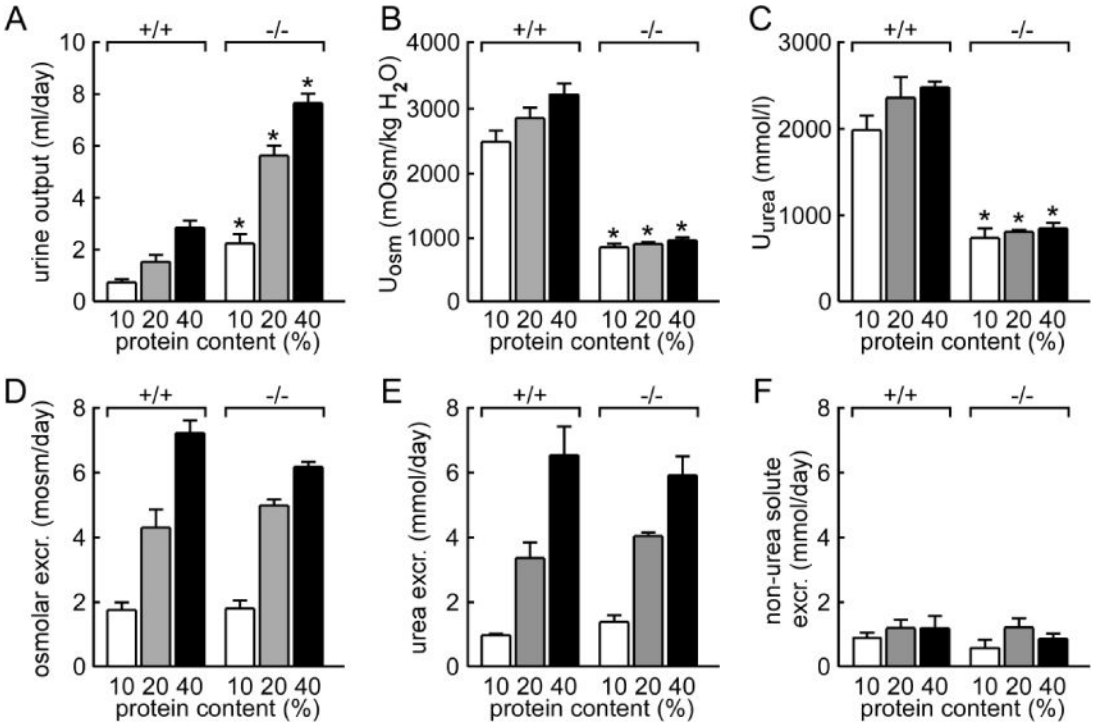

Fig. 4. Renal handling of long term urea loading in mice fed diets containing 10, 20, or 40% protein

A. urine output. **B.** urinary osmolality (U_{osm}). **C.** urinary urea concentration (U_{urea}). **D.** urinary osmolar excretion (Osmolar excr.). **E.** urea excretion. **F.** excretion of non-urea solutes. Data are presented as means ± SEM. n = 6. *p < 0.05 *vs.* wild-type mice.

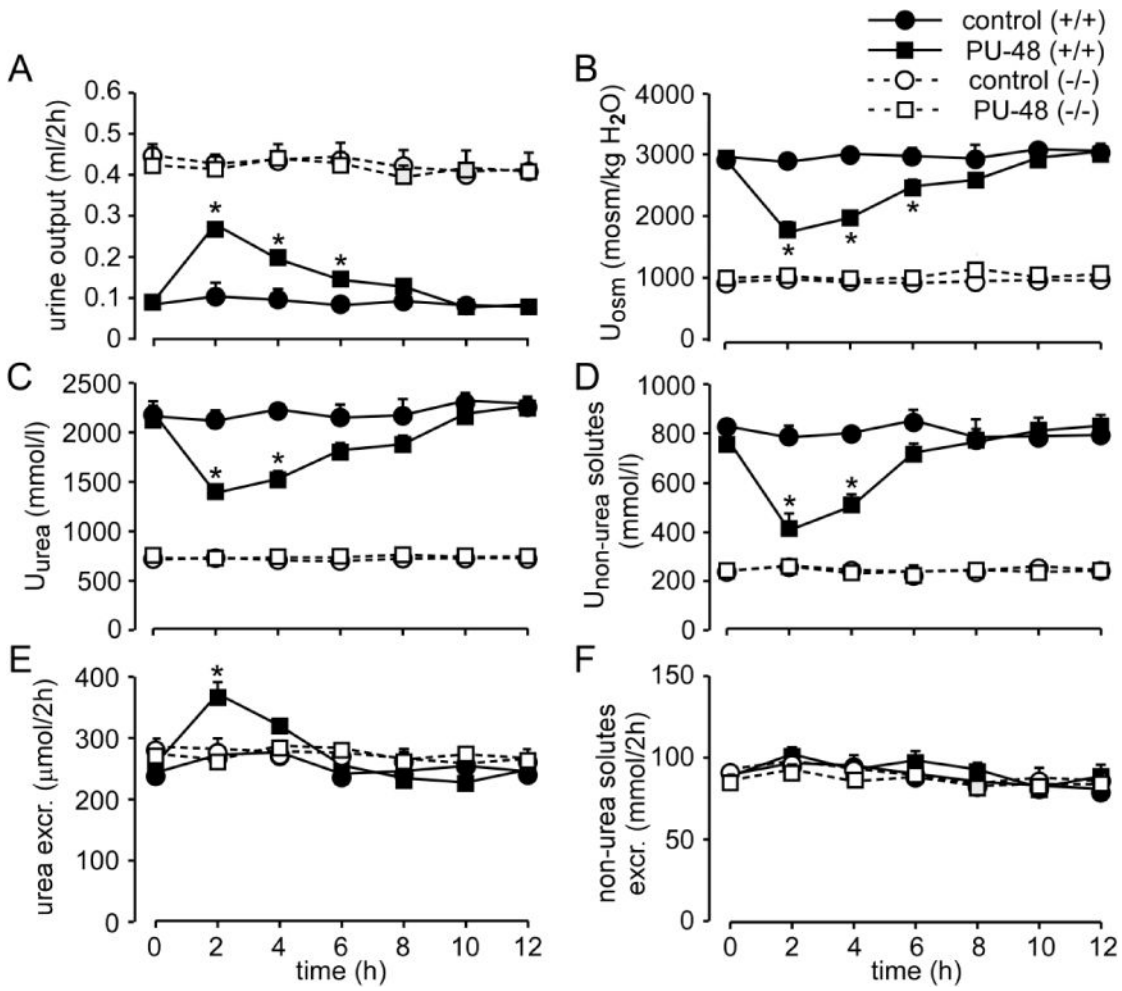

Fig. 5. Diagram of urea recycling in the kidney of wild-type (A) and all-UT-knockout mice (B)
Urea flows are indicated by blue arrows. See text for details.

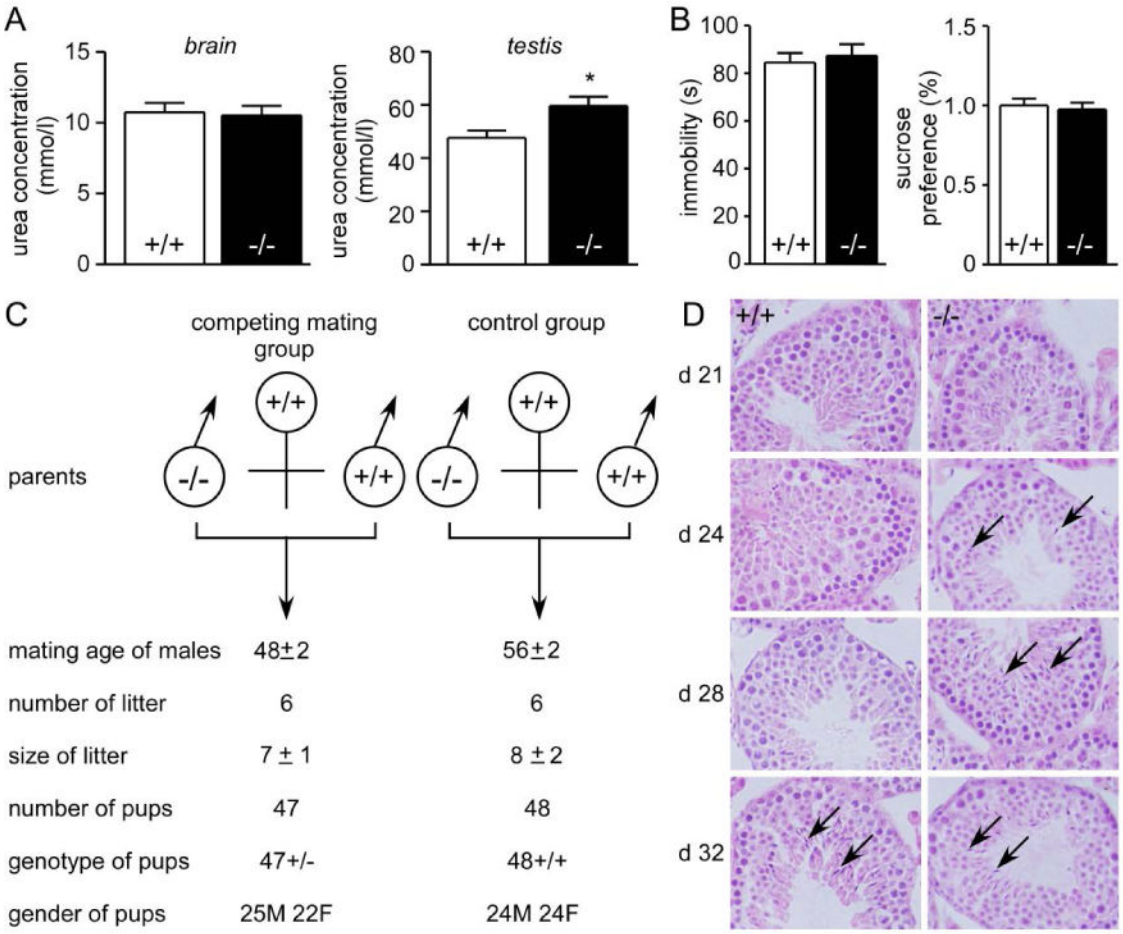

Fig. 6. Determination of selective inhibition of PU-48 on UTs

Wild-type and UT-B null mice were observed in metabolic cages and subcutaneously injected with or without 100 mg/kg of PU-48 just after a 2-h urine collection (time 0). Urine samples were collected every 2 h. **A.** urine output. **B.** urinary osmolality (U_{osm}). **C.** urine urea concentration (U_{urea}). **D.** urine non-urea concentration ($U_{non\text{-}urea}$). **E.** urea excretion. **F.** excretion of non-urea solutes. Data are presented as means ± SEM. n = 6. *p < 0.05 *vs.* wild-type mice.

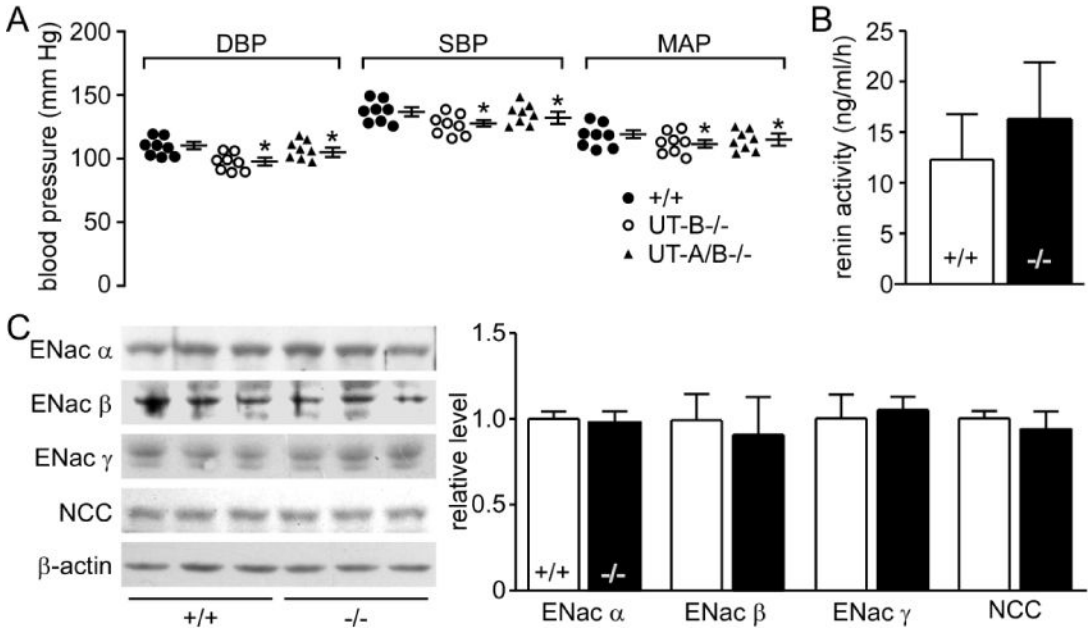

Fig. 7. Extra renal phenotypes of all-UT-knockout mice

A. *left*, forced swim test. Data are presented as means ± SEM. n = 10. *p < 0.05 *vs.* wild-type mice. *right*, sucrose preference test. Data are presented as means ± SEM. n = 10*. P < 0.05 *vs.* wild-type mice. **B**. blood pressure. DBP, Diastolic blood pressure; SBP, systolic blood pressure; MAP, mean arterial pressure. Data are presented as means ± SEM. n = 8. **C.** HE staining of testis tissue sections. **D.** breeding performance of maturing male mice. Male (M) mice at 4-week-old were housed with 8-week-old wild-type female (F) mice. Data are shown for 6 pairs of competing mates (left) and 6 pairs of wild-type controls (right) and are means ± SEM.

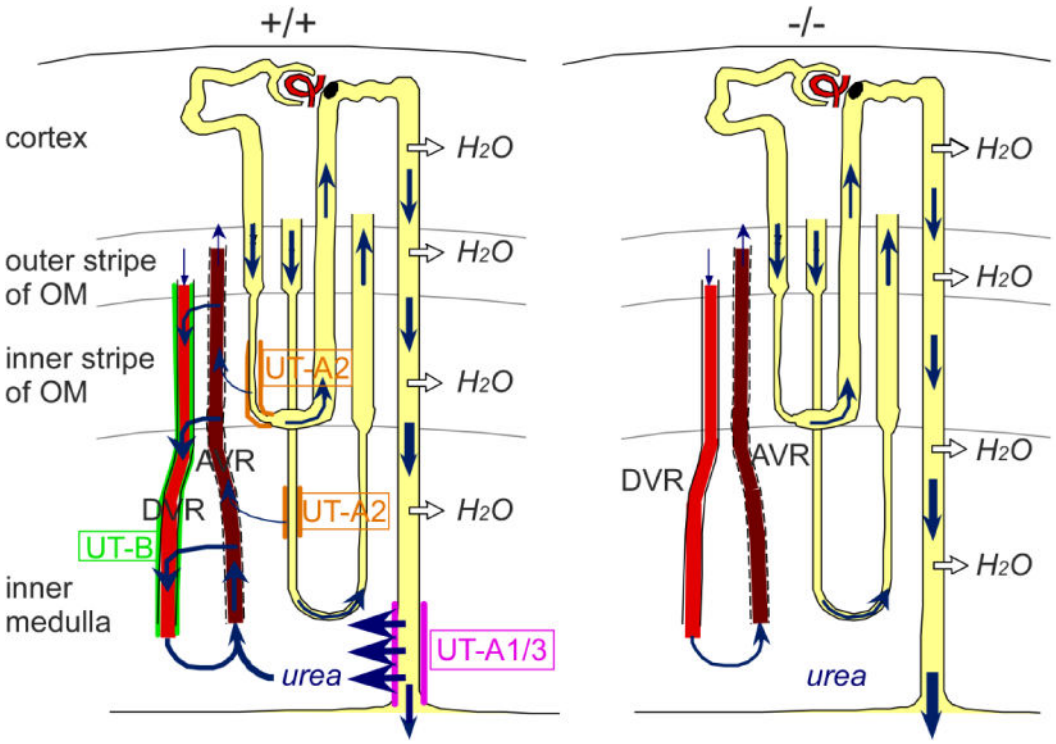

Fig. 8. Diagram of urea recycling in the kidney of wild-type and all-UT-knockout mice

Urea flows are indicated by blue arrows.

Table 1

Blood and urinary chemistry in wild-type (WT) and all-UT-knockout (KO) mice

	WT	KO	KO/WT
Body weight, g	26.0±0.4	25.6±0.5	0.98
Urine			
Urine output, ml/day	1.8±0.2	6.4±0.4*	3.55
Urine osmolality, mosm/kg H_2O	2503±85	941±53*	0.37
Urine urea concentration, mmol/L	2253±57	797±39*	0.35
Urine creatinine concentration, mmol/L	16.4±0.9	5.2±0.4*	0.31
Osmolar excretion, osm/day	5.6±0.4	5.3±0.3	0.95
Urea excretion, mmol/day	3.9±0.6	4.3±0.2	1.1
Plasma and clearances			
Plasma urea concentration, mmol/L	9.2±0.3	9.9±0.7	1.07
Plasma creatinine concentration, μmol/L	35±0.9	37±0.8	1.06
Plasma potassium concentration, mmol/L	6.9±0.2	6.9±0.2	1
Plasma sodium concentration, mmol/L	156±0.8	156±1.3	1
Plasma chloride concentration, mmol/L	110±0.4	111±1	1.01
Plasma calcium concentration, mmol/L	2.5±0.1	2.6±0.1	1.04
Urea clearance, ml/day	441±26	512±41	1.16
Creatinine clearance, ml/day	842±39	896±47	1.06
Urea clearance/creatinine clearance	0.52±0.01	0.57±0.01	1.09
Urine-to-plasma ratios			
U/P_{urea}	245±37	80±21*	0.32
$U/P_{creatinine}$	468±32	140±17*	0.30
Plasma lipid			
Plasma TG concentration, mmol/L	1.23±0.08	1.31±0.16	1.06
Plasma HDL concentration, mmol/L	1.13±0.04	1.30±0.10	1.15
Plasma HDL concentration, mmol/L	0.21±0.01	0.18±0.01	0.85

Values are means±SE of 6 mice/group.

* $P<0.05$ compared with WT mice.

Table 2

Urine concentrating ability in different UT knockout mice

	Urine output (ml/day)	Urinary urea (mmol/l)	Urea excretion (mmol/day)	Urinary osmolality (mosm/kg H_2O)	Osmolality excretion (osm/day)	Urinary Non-urea solutes (mmol/l)	Non-urea solutes excretion (mmol/day)	Medulla osmolality (mosm/l)
WT	1.5	1472	2.2	2288	3.4	816	1.22	340
UT-B KO	2.4	797	1.9	1318	3.2	521	1.25	171
UT-A1/3 KO	5	799	3.9	861	4.3	62	0.31	86
UT-A2 KO	1.5			2052	3.1			
UT-A2/B KO	1.8	1205	2.2	1775	3.2	570	1.03	302
UT-A3 KO	1.8	1286	2.3	2246	4.0	960	1.72	
All-UT KO	6.4	797	5.1	941	6.0	144	0.92	77

WT, wild-type; KO, knockout. Data were derived from the references [5, 30, 34, 35 and 52]. Data for WT are mean value from references [5, 30, 35, 52].

Table 3

Model predictions for wild-type (WT) and different UT knockout (KO) rat

	WT	UT-B KO	UT-A1/3 KO	UT-A2 KO	All-UT KO
DVR urea flow (mol/day)	1.43	0.93	1.06	1.57	0.61
DVR flow (ml/day)	49.1	45.8	49.5	49.1	47.8
DVR osmolality (mosm/(kgH_2O))	615	631	607	619	611
CD urea flow (mol/day)	7.0	6.9	6.8	7.0	6.7
CD urea concentration (mmol/l)	317	317	309	319	308
CD osmolality (mosm/(kgH_2O))	779	786	779	783	782
Interstitial fluid urea concentration (mmol/l)	560	549	172	560	113
Urea excretion (mmol/day)	2.1	1.9	5.8	2.1	5.7
Urine flow (ml/day)	3.8	4.0	11.3	3.8	11.5
Urine urea (mmol/l)	563	551	513	563	494
Urine osmolality (mosm/(kgH_2O))	1197	1176	789	1197	772

Flow values given per kidney. CD, collecting duct; DVR, descending vasa recta; OM, outer medulla; IM, inner medulla.